



# A new colorimetric and fluorescent ratiometric sensor for $\text{Hg}^{2+}$ based on 4-pyren-1-yl-pyrimidine

Jiena Weng, Qunbo Mei\*, Qidan Ling, Quli Fan, Wei Huang\*

Key Laboratory for Organic Electronics and Information Displays (KLOEID), Institute of Advanced Materials (IAM), Nanjing University of Posts and Telecommunications, Nanjing 210046, China

## ARTICLE INFO

### Article history:

Received 24 October 2011  
Received in revised form 15 December 2011  
Accepted 23 December 2011  
Available online 28 December 2011

### Keywords:

Chemosensor  
 $\text{Hg}^{2+}$   
Pyrene  
Pyrimidine

## ABSTRACT

A novel fluorescent ratiometric chemosensor based on 4-pyren-1-yl-pyrimidine (**PPM**) has been designed and prepared for the detection of  $\text{Hg}^{2+}$  in the presence of other competing metal ions in acetonitrile. The photo exhibits fluorescence color change of **PPM** from blue to green without and with  $\text{Hg}^{2+}$ , which red shift of wavelength about 105 nm in fluorescence emission spectra. It can serve as a highly selective chemodosimeter for  $\text{Hg}^{2+}$  with ratiometric and naked-eye detection. The photophysical properties of **PPM** confirmed a 2:1 (**PPM**– $\text{Hg}^{2+}$ ) binding model and the spectral response toward  $\text{Hg}^{2+}$  was proved to be reversible.

© 2012 Elsevier Ltd. All rights reserved.

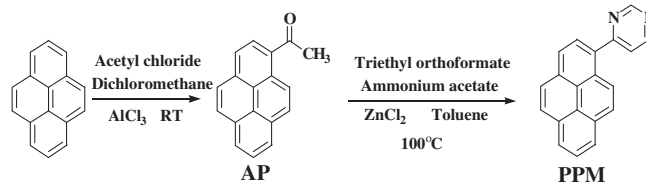
## 1. Introduction

Currently, there is great interest in the development of highly selective and sensitive fluorescent sensors for quantifying and exploring the heavy and transition metal ions in biology and in the environment.<sup>1</sup> Among these metal ions, mercury(II) has attracted considerable attention due to its toxicity to environment and biological systems.<sup>2</sup> For the past few years, many studies have been reported on the design and synthesis of chemosensors for detecting  $\text{Hg}^{2+}$ .<sup>3</sup> However, most of these chemosensors molecular to monitor metal ions are often structurally complicated and require sophisticated synthetic process. As a result, considerable efforts have been devoted to design new and practical chemosensors for  $\text{Hg}^{2+}$  detection.

As fluorophores, pyrene moiety is one of the most useful scaffolds for the construction of fluorogenic chemosensors for a variety of important chemical species.<sup>4</sup> Depending on the relative proximity between pyrene moieties, efficient, and sensitive monomer emission at 370–430 nm and excimer emission around 480 nm are observed.<sup>5</sup> Upon coordination with a specific guest ion, the host molecule could be fine-tuned to yield monomer and/or excimer emissions depending on the orientation of the two pyrene moieties.<sup>6</sup> Many investigations have been conducted to fabricate ratiometric fluorescent sensors for  $\text{Hg}^{2+}$ ,  $\text{Cu}^{2+}$ ,  $\text{Zn}^{2+}$ ,  $\text{Cd}^{2+}$ , and  $\text{Ag}^+$  etc., by introducing two pyrene moieties and utilizing the pyrene

moiety of monomer versus excimer.<sup>7</sup> However, as far as we know, only a few ratiometric fluorescent probes with one pyrene moiety for metal ions have been found in the literature until now.<sup>8</sup>

Theoretically, fluorescent chemosensors consist of ion recognition unit attached with a fluorogenic unit. The recognition unit is responsible for the selectivity and binding efficiency of the chemosensor.<sup>9</sup> As a result, while designing sensors the recognition unit linked to fluorophore should be carefully examined. Many heterocycle, such as pyridine, quinoline, triazole, thiazole, pyrrole, or imidazole etc., and their derivatives are utilized as recognition unit.<sup>10</sup> Pyrimidine is one of the important heterocycle with a variety of biological and medicinal activities,<sup>11</sup> and some of pyrimidine derivatives are applied as photoelectric materials recently.<sup>12</sup> However, the research using pyrimidine as recognition unit in chemosensor has not yet been reported. Herein, we describe a new ratiometric fluorescent probe with one pyrene moiety for metal ions, using pyrimidine as recognition unit. The new pyrimidine–pyrene derivative chemosensor **PPM** (Scheme 1) shows a selective, sensitive, and reversible fluorescence change response to the  $\text{Hg}^{2+}$ .



Scheme 1. Synthetic route for **PPM**.

\* Corresponding authors. Tel.: +86 25 8586 6008; fax: +86 25 8586 6999; e-mail addresses: iamqbmei@njupt.edu.cn (Q. Mei), iamwhuang@njupt.edu.cn, iamdirector@fudan.edu.cn (W. Huang).

## 2. Results and discussion

The synthetic route for **PPM** is shown in Scheme 1. The intermediate compound **AP** was synthesized from pyrene by classical Friedel–Crafts reaction in 62% yield. **PPM** was synthesized by ZnCl<sub>2</sub>-catalyzed three-component coupling reaction in 21% yield.<sup>13</sup> The structure of the products was identified by using <sup>1</sup>H NMR, <sup>13</sup>C NMR, and GC–MS.

The chemosensor **PPM** displayed sensitive fluorescence change via pyrimidine ring chelating with Hg<sup>2+</sup>. Addition of 2 equiv of various alkali, alkaline earth, and transition metal ions (Na<sup>+</sup>, K<sup>+</sup>, Mg<sup>2+</sup>, Ag<sup>+</sup>, Cd<sup>2+</sup>, Co<sup>2+</sup>, Cr<sup>3+</sup>, Cu<sup>2+</sup>, Fe<sup>3+</sup>, Hg<sup>2+</sup>, Ni<sup>2+</sup>, Pb<sup>2+</sup>, Zn<sup>2+</sup>) to a solution of **PPM** (*c*=1.25×10<sup>−4</sup> M) in acetonitrile showed a selective fluorescence change from blue to green only in case of Hg<sup>2+</sup> (Fig. 1). This selective fluorescence change with **PPM** can be used for the fluorescence detection of Hg<sup>2+</sup> in solution (Fig. 1). Similar fluorescence change was also observed with Hg<sup>2+</sup> in the presence of other ions in this study.

Detailed optical studies were carried out to establish the selective sensing between Hg<sup>2+</sup> and **PPM** in acetonitrile. Because this small organic molecule displayed not only absorption but also emission variations depending on the metal ion present, so UV–vis and fluorescence measurements were investigated.

The absorption spectra of **PPM** in acetonitrile was typical of those for other *N*-heterocycles with covalently bound pyrenyl groups.<sup>14</sup> As showed in Fig. 2, a long-wavelength absorption for a pyrenyl-based π–π\* transition was found centered at 350 nm, while the heterocyclic (pyrimidine)-based π–π\* transition was centered at 279 nm. The chemosensor behavior in the presence of 2 equiv of different metal ions (Na<sup>+</sup>, K<sup>+</sup>, Mg<sup>2+</sup>, Ag<sup>+</sup>, Cd<sup>2+</sup>, Co<sup>2+</sup>, Cr<sup>3+</sup>, Cu<sup>2+</sup>, Fe<sup>3+</sup>, Hg<sup>2+</sup>, Ni<sup>2+</sup>, Pb<sup>2+</sup>, Zn<sup>2+</sup>) indicated that only Hg<sup>2+</sup> promoted a notable response in its absorption spectra (Fig. 3). Upon addition of Cr<sup>3+</sup> and Fe<sup>3+</sup>, although a weak new peak at 430 nm was observed, the typical absorption of **PPM** at 244 nm, 279 nm, and 350 nm showed slight change in UV–vis spectra.

Upon addition of Hg<sup>2+</sup>, two strong new peaks at 300 nm and 415 nm were observed, with the peaks at 279 nm and 350 nm disappeared. The peak at 415 nm in the case of Hg<sup>2+</sup> could be attributed to the formation of **PPM**–Hg<sup>2+</sup> chelating complex. The Job's plot (Fig. 4) for **PPM** titrated with Hg<sup>2+</sup> revealed a 2:1 stoichiometry of the complexation species.

Systematic spectrophotometric titration with increasing [Hg<sup>2+</sup>] revealed a gradual decrease of absorption band centered at 350 nm with the concomitant increase in a new low-energy band centered at 415 nm (Fig. 5). The spectra remained constant after adding approximately 3 equiv of Hg<sup>2+</sup>. The well-defined isosbestic points at 322 nm and 369 nm clearly indicated the presence of a unique complex in equilibrium with the free ligand. The new low-energy band, which was red-shifted 65 nm, was responsible for the change of color from colorless to yellow (inset of Fig. 5). In order to confirm the stoichiometry of the formed complex, another titration was carried out with increasing **PPM** (Fig. S2). From the analysis of the absorption spectral data (Fig. 6), the binding of Hg<sup>2+</sup> also confirmed the formation of 2:1 (**PPM**–Hg<sup>2+</sup>) chelating complex, and occurred in a ratiometric manner through a weakened **PPM**

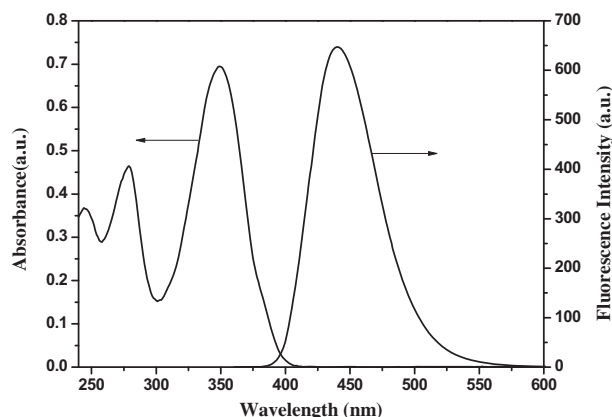


Fig. 2. UV–vis and fluorescence spectra ( $\lambda_{\text{ex}}=370$  nm) of **PPM** in acetonitrile ( $c=5.0\times 10^{-5}$  M).

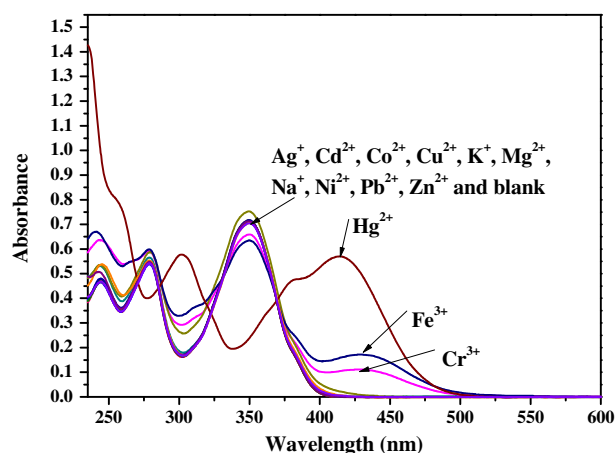


Fig. 3. UV–vis spectra of **PPM** ( $c=5.0\times 10^{-5}$  M) in the presence of metal ions in acetonitrile. Ag<sup>+</sup>, Cd<sup>2+</sup>, Co<sup>2+</sup>, Cr<sup>3+</sup>, Cu<sup>2+</sup>, Fe<sup>3+</sup>, Hg<sup>2+</sup>, Mg<sup>2+</sup>, Ni<sup>2+</sup>, Na<sup>+</sup>, Pb<sup>2+</sup>, and Zn<sup>2+</sup> ions (2.0 equiv) were added, respectively.

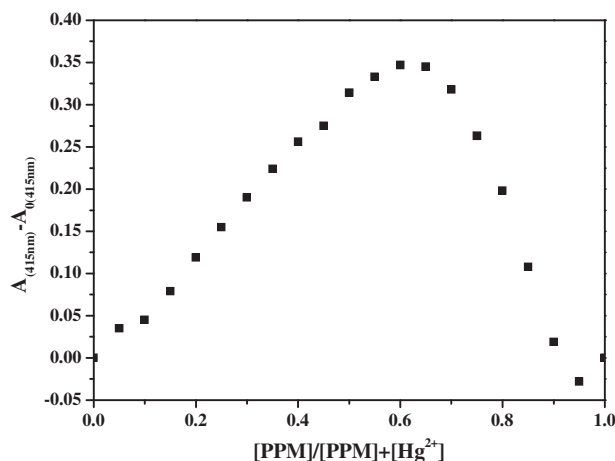


Fig. 4. Job's plot for evaluation of the 2:1 binding stoichiometry between **PPM** and Hg(ClO<sub>4</sub>)<sub>2</sub> in acetonitrile medium; the total [**PPM**]+[Hg<sup>2+</sup>]=5.0×10<sup>−5</sup> M.

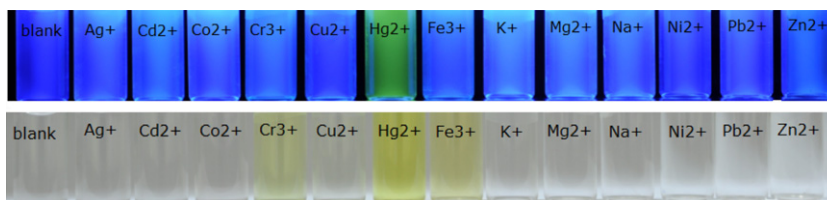
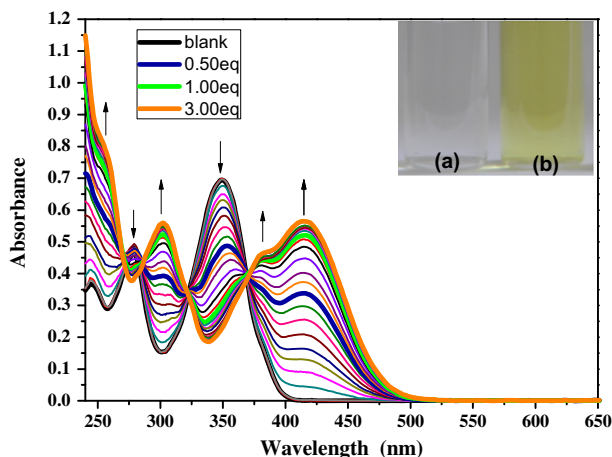


Fig. 1. Changes in the color of **PPM** ( $c=5.0\times 10^{-5}$  M) with 2 equiv of various metal ions in acetonitrile. Top: color changes by exciting at 360 nm; bottom: color changes for 'naked-eye'.



**Fig. 5.** UV-vis spectra of **PPM** in acetonitrile ( $c=5.0 \times 10^{-5}$  M) in the presence of increasing amount of  $\text{Hg}(\text{ClO}_4)_2$  (0–3.0 equiv) predissolved in acetonitrile. Arrows indicate the absorptions that increase (up) and decrease (down) during the titration experiments. Inset: change in the color of **PPM** after addition of 2 equiv of  $\text{Hg}(\text{ClO}_4)_2$ , **PPM** in acetonitrile (a) and **PPM** plus 2 equiv of  $\text{Hg}(\text{ClO}_4)_2$  in acetonitrile (b).

and ascending complex emission, which made it possible to ratiometrically detect  $\text{Hg}^{2+}$ .

**PPM** showed very strong fluorescence in acetonitrile (Fig. 1). The emission spectrum displayed typical emission bands centered

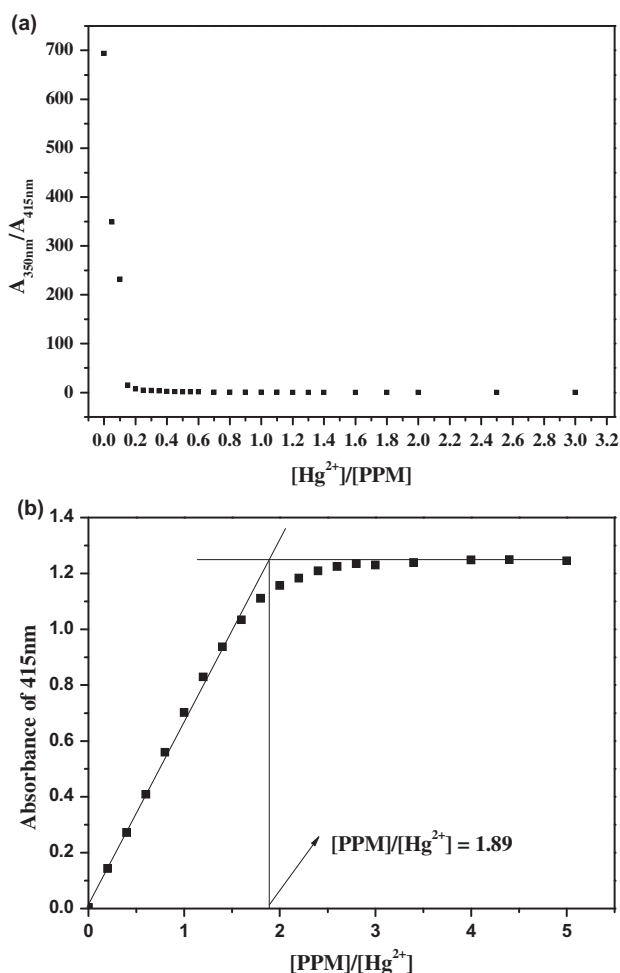


**Fig. 6.** (a): The ratios of absorption at 350 nm to those at 415 nm ( $A_{350\text{nm}}/A_{415\text{nm}}$ ) depended on the ratios of  $[\text{Hg}^{2+}]/[\text{PPM}]$  upon addition  $\text{Hg}(\text{ClO}_4)_2$  into a solution of **PPM** ( $c=5.0 \times 10^{-5}$  M); (b): The variation of absorption at 415 nm depended on the ratios of  $[\text{PPM}]/[\text{Hg}^{2+}]$  upon addition **PPM** into a solution of  $\text{Hg}(\text{ClO}_4)_2$  ( $c=5.0 \times 10^{-5}$  M).

at 440 nm with a high quantum yield ( $\Phi=1.00$ ). It was interesting that the emission spectrum of **PPM** recorded at different concentration in acetonitrile did not show any red-shifted emission (Fig. S3). Sharp concentration quenching of emission at high concentration ( $c=1.0 \times 10^{-3}$  M) for **PPM** but with no concomitant red shift in emission spectra, which indicated that **PPM** was monomeric in dilute acetonitrile solution rather than being associated via inter-molecular  $\pi$ -stacking interactions.

The fluorescence behavior of **PPM** in the presence of the  $\text{Hg}^{2+}$  was examined. Upon gradual addition of  $\text{Hg}^{2+}$  (0–0.5 equiv) to the solution of **PPM** in acetonitrile ( $c=5.0 \times 10^{-5}$  M), the intensity of the emission band centered at 440 nm decreased gradually and that of a new fluorescent band centered at 545 nm increased gradually, which was attributed to the formation of **PPM**– $\text{Hg}^{2+}$  complex (Fig. 7). As a result, an obvious change in fluorescent color from blue to green was observed (inset of Fig. 7). The more addition of  $\text{Hg}^{2+}$  (0.6–3.0 equiv), caused fluorescent quenching and showed a steady and smooth decrease both at 410 nm and 545 nm (inset of Fig. 7). Fitting of the titration curve also suggested a 2:1 stoichiometry **PPM**– $\text{Hg}^{2+}$  complexation species. According to the literature,<sup>15</sup> the detection limit was also estimated from the titration results and was  $4.69 \times 10^{-6}$  M.

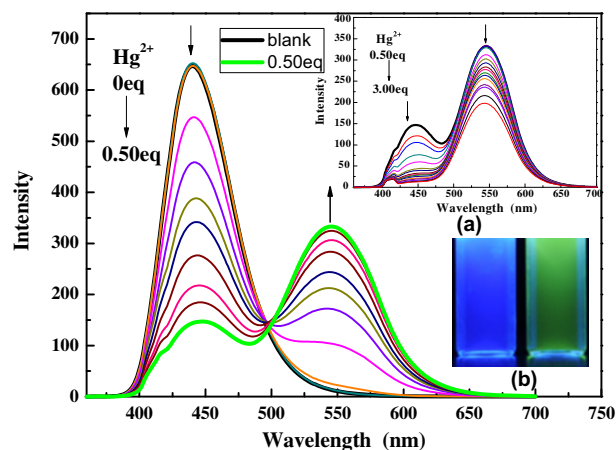


**Fig. 7.** Fluorescence spectra of **PPM** in acetonitrile ( $5.0 \times 10^{-5}$  M,  $\lambda_{\text{ex}}=400$  nm) in the presence of increasing amount of  $\text{Hg}(\text{ClO}_4)_2$  (0–0.5 equiv) predissolved in acetonitrile. Insets: (a) fluorescence spectra of **PPM** in the presence of increasing amount of  $\text{Hg}(\text{ClO}_4)_2$  (0.5–3.0 equiv). (b) Change in the fluorescence of **PPM** after addition of 2 equiv of  $\text{Hg}(\text{ClO}_4)_2$ . From left to right, **PPM** in acetonitrile and **PPM** plus 2 equiv of  $\text{Hg}(\text{ClO}_4)_2$  in acetonitrile.

To explore practical applicability of **PPM** as a  $\text{Hg}^{2+}$  selective chemosensor, a competition experiment was done. As showed in Fig. 8, under the same condition slight fluorescence changes of **PPM** were observed in the presence of 2 equiv of different metal ions ( $\text{Na}^+$ ,  $\text{K}^+$ ,  $\text{Mg}^{2+}$ ,  $\text{Ag}^+$ ,  $\text{Cd}^{2+}$ ,  $\text{Co}^{2+}$ ,  $\text{Ni}^{2+}$ , and  $\text{Pb}^{2+}$ ). By addition of transition metal ions ( $\text{Cu}^{2+}$ ,  $\text{Cr}^{3+}$ ,  $\text{Fe}^{3+}$ ), the fluorescent intensity of **PPM** decreased to varying degrees, especially the addition of 2 equiv of  $\text{Cr}^{3+}$  or  $\text{Fe}^{3+}$  caused about 43% or 53% fluorescence decrease of **PPM**, respectively, but no any new emission band was observed. And the addition of 2 equiv of  $\text{Zn}^{2+}$  caused a shoulder band centered at 491 nm (Fig. S4); however, the intensity of the peak at 440 nm decreased only 3%. A great difference between addition of 2 equiv of  $\text{Hg}^{2+}$  and other metal ions was not only the emission band centered at 440 nm disappeared almost, but also a new band centered at 545 nm appeared. Thus **PPM** was more sensitively to detect  $\text{Hg}^{2+}$  than other metal ions mentioned above. Further more, upon addition of 2 equiv of  $\text{Hg}^{2+}$  to the solution, which containing **PPM** and 2 equiv of competing metal ion, the change of the emission was similar to that only 2 equiv of  $\text{Hg}^{2+}$  was

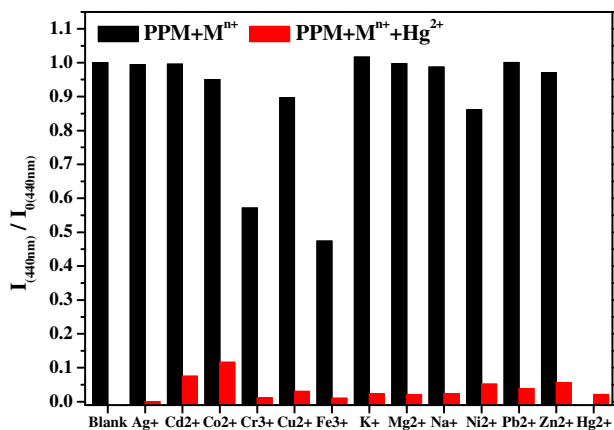


**Fig. 8.** Fluorescence responses of **PPM** in acetonitrile ( $5.0 \times 10^{-5}$  M,  $\lambda_{\text{ex}}=400$  nm) to various 2 equiv of metal ions. Bars represent the final ( $I_{(440\text{nm})}$ ) over the initial ( $I_{0(440\text{nm})}$ ) emission intensity. The black bars represent the addition of the competing metal ion to the solution of **PPM**. The red bars represent the change of the emission that occurs upon the subsequent addition of 2 equiv of  $\text{Hg}^{2+}$  to the above solution.

added to the **PPM** solution. As a result, **PPM** displayed selectivity to detect  $\text{Hg}^{2+}$ .

Reversibility and regeneration are important factors for chemosensor in practical applications.<sup>16</sup> Because  $\text{I}^-$  has strong binding ability toward  $\text{Hg}^{2+}$ , KI was added to the solution of **PPM**– $\text{Hg}^{2+}$  species to test whether the proposed complex could be reversed. The introduction of KI (2 equiv to  $\text{Hg}^{2+}$ ) could immediately restore the initial fluorescence of **PPM**. When  $\text{Hg}^{2+}$  (1 equiv to **PPM**) was added to system again, the fluorescence of **PPM** was quenched (Fig. S6–S8). The regeneration indicated that the chemosensor **PPM** could be revived with proper treatment. This process could be repeated at least ten times (Fig. 9), which signified that **PPM** can function as a fluorescent switch modulated by  $\text{Hg}^{2+}$ /KI (Fig. 9).

For our system, there were two potential binding sites in the pyrimidine ring, however, all the analysis mentioned-above confirmed a 2:1 (**PPM**– $\text{Hg}^{2+}$ ) binding model, thus it might be suggested that only one of the nitrogen atoms in **PPM** operated. In order to study the complexation mode of  $\text{Hg}^{2+}$  with **PPM**, a comparison of  $^1\text{H}$  NMR experiments of **PPM** with those of **TPAPM** (diphenyl-(4-pyrimidin-4-yl-phenyl)-amine)<sup>17</sup> and **PPy** (2-phenylpyridine) were carried out. We performed  $^1\text{H}$  NMR experiments in ( $\text{DMSO}-d_6$ ), which were shown in Fig. 10 and Fig. S9. Upon addition of excessive  $\text{Hg}^{2+}$ , considerable change was noted in the chemical shift of  $\text{H}_c$  in the pyrimidine group of **PPM**, which shifted to downfield by 0.19 ppm. The proton signal of  $\text{H}_d$  in the pyrene ring

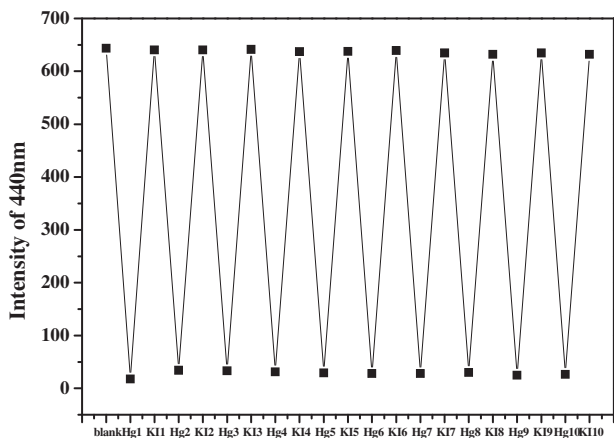


**Fig. 9.** Fluorescence intensity changes of **PPM** in acetonitrile ( $5.0 \times 10^{-5}$  M,  $\lambda_{\text{ex}}=400$  nm) upon alternate addition of  $\text{Hg}(\text{ClO}_4)_2$  and KI.

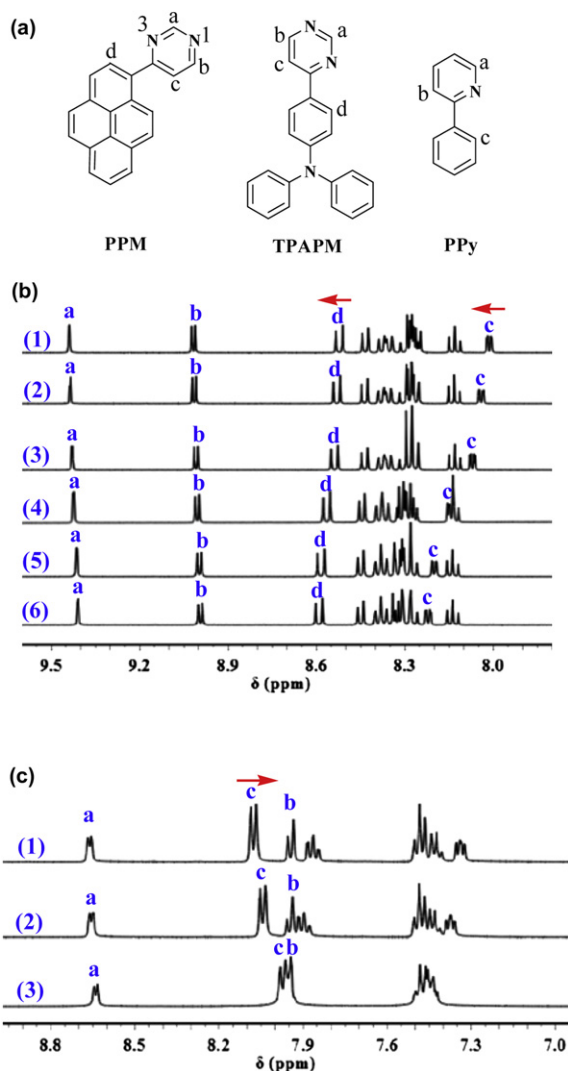
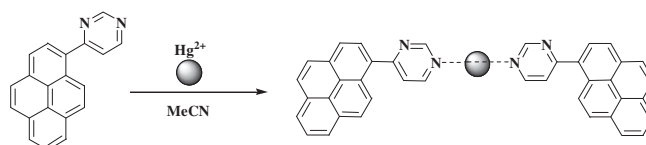


**Fig. 10.** (a) Molecular structure formulas of **PPM**, **TPAPM**, and **PPy**; (b) The  $^1\text{H}$  NMR spectra of (1) **PPM** in  $\text{DMSO}-d_6$ ; (2)–(6) upon gradual addition of solid  $\text{Hg}(\text{ClO}_4)_2$  to the solution of **PPM** in  $\text{DMSO}-d_6$ ; (c) The  $^1\text{H}$  NMR spectra of (1) **PPy** in  $\text{DMSO}-d_6$ ; (2)–(3) upon gradual addition of solid  $\text{Hg}(\text{ClO}_4)_2$  to the solution of **PPy** in  $\text{DMSO}-d_6$ .

was also shifted to downfield slightly. In the case of **TPAPM**, the changes of chemical shift were almost the same as those of **PPM**. However, treatment of excessive  $\text{Hg}^{2+}$ , the proton signal of  $\text{H}_b$  in the pyridine group of **PPy** has nearly no change. Another difference between **PPy** and **PPM** in the  $^1\text{H}$  NMR experiments was that the proton signal of  $\text{H}_c$  in the phenyl of **PPy** shifted to upfield obviously. These spectral changes might be suggested that  $\text{Hg}^{2+}$  was bound to the 1-position nitrogen atom rather than the 3-position nitrogen atom. Based on the result of the  $^1\text{H}$  NMR experiments, the possible binding mechanism of **PPM** with  $\text{Hg}^{2+}$  was schematically depicted in Scheme 2. Moreover, the formation of new chelating complex between **PPM** and  $\text{Hg}^{2+}$  can be proved by the appearance of new absorption band as well as red-shift emission band in UV–vis spectra and fluorescence emission spectra, respectively.



**Scheme 2.** The possible binding mechanism of **PPM** with  $\text{Hg}^{2+}$ .

### 3. Conclusion

In summary, we have developed a novel fluorescent sensor for  $\text{Hg}^{2+}$  based on the 4-pyren-1-yl-pyrimidine (PPM) with high sensitivity and selectivity. This chemosensor was easily prepared and found to be possible to detect the  $\text{Hg}^{2+}$  ratiometrically. The remarkable photophysical properties of PPM confirmed a 2:1 (PPM– $\text{Hg}^{2+}$ ) binding model and the spectral response toward  $\text{Hg}^{2+}$  was established to be reversible. More interestingly, the  $\text{Hg}^{2+}$  was bound to the 1-position nitrogen atom of PPM, which has been proposed on the basis of  $^1\text{H}$  NMR experiments. This work opens up the possibility of a family of highly sensitive chemosensors for  $\text{Hg}^{2+}$  based on 4-aryl-pyrimidine.

### 4. Experimental

#### 4.1. Materials and instrumentations

Acetonitrile was of high performance liquid chromatography purity and used without further treatment. All other solvents and reagents were of analytical purity and used without further purification. The salts solutions of metal ions were  $\text{NaNO}_3$ ,  $\text{KNO}_3$ ,  $\text{Mg}(\text{ClO}_4)_2$ ,  $\text{AgNO}_3$ ,  $\text{Cd}(\text{NO}_3)_2 \cdot 4\text{H}_2\text{O}$ ,  $\text{Co}(\text{NO}_3)_2 \cdot 6\text{H}_2\text{O}$ ,  $\text{Cr}(\text{NO}_3)_3 \cdot 9\text{H}_2\text{O}$ ,  $\text{Cu}(\text{NO}_3)_2 \cdot 3\text{H}_2\text{O}$ ,  $\text{Fe}(\text{NO}_3)_3 \cdot 9\text{H}_2\text{O}$ ,  $\text{Hg}(\text{ClO}_4)_2 \cdot 3\text{H}_2\text{O}$ ,  $\text{Ni}(\text{NO}_3)_2 \cdot 6\text{H}_2\text{O}$ ,  $\text{Pb}(\text{NO}_3)_2$ ,  $\text{Zn}(\text{NO}_3)_2 \cdot 6\text{H}_2\text{O}$ .  $^1\text{H}$  NMR and  $^{13}\text{C}$  NMR were measured on a Bruker Ultra Shield Plus 400 MHz spectrometer with TMS as an internal standard and  $\text{CDCl}_3/\text{DMSO}-d_6$  as solvent. Mass spectrometric data were obtained with a Shimadzu GC-MS-QP 2010 Plus spectrometry. UV–vis spectra were recorded on a Shimadzu UV-3600 UV–vis-NIR spectrophotometer. Fluorescence spectra were determined with Shimadzu RF-5301PC luminescence spectrometer.

#### 4.2. General procedures of spectra detection

Solutions of  $\text{Fe}^{3+}$ ,  $\text{Cr}^{3+}$ ,  $\text{Pb}^{2+}$  were prepared in mixed solvent of acetonitrile and deionized water ( $V_{\text{acetonitrile}}/V_{\text{deionized water}}=9:1$ ). Solutions of all other metal ions were prepared in acetonitrile. The solutions of PPM and KI were also prepared in acetonitrile. In titration experiments, each time a 3 mL solution of PPM was filled in a quartz optical cell of 1 cm optical path length, and the  $\text{Hg}^{2+}$  solution was added into quartz optical cell gradually by using a micro-pipette. Spectral data were recorded at 3 min after the addition.

#### 4.3. Quantum yield measurement

Fluorescence quantum yield was determined using optically matching solutions of 9,10-diphenylanthracene ( $\Phi_f=0.9$  in cyclohexane) as standards at an excitation wavelength of 360 nm and the quantum yield is calculated using Eq. 1.<sup>18</sup>

$$\Phi_{\text{unk}} = \Phi_{\text{std}} \left( \frac{I_{\text{unk}}/A_{\text{unk}}}{I_{\text{std}}/A_{\text{std}}} \right) \left( \frac{\eta_{\text{unk}}}{\eta_{\text{std}}} \right)^2 \quad (1)$$

Where  $\Phi_{\text{unk}}$  and  $\Phi_{\text{std}}$  are the fluorescence quantum yields of the sample and the standard, respectively.  $I_{\text{unk}}$  and  $I_{\text{std}}$  are the integrated emission intensities of the sample and the standard, respectively.  $A_{\text{unk}}$  and  $A_{\text{std}}$  are the absorbance of the sample and the standard, respectively. And  $\eta_{\text{unk}}$  and  $\eta_{\text{std}}$  are the refractive indexes of the corresponding solutions.

#### 4.4. Synthesis

**4.4.1. 1-Pyren-1-yl-ethanone (AP).** A mixture of  $\text{AlCl}_3$  (2.95 g, 22 mmol), acetyl chloride (1.6 mL, 22 mmol) in  $\text{CH}_2\text{Cl}_2$  (50 mL) was added dropwise to a solution of pyrene (4.04 g, 20 mmol) in  $\text{CH}_2\text{Cl}_2$

(100 mL) at 0 °C. The mixture was stirred at room temperature over night. The mixture was poured into 1 L deionized water slowly and stirred for 2 h. And then, the mixture was separated, the organic layer was collected, dried over anhydrous  $\text{MgSO}_4$ , filtrated, and concentrated. The residue was purified by silica gel column chromatography to give the compound AP (3.02 g, 62%) as light yellow solid.  $^1\text{H}$  NMR (400 MHz,  $\text{CDCl}_3$ ):  $\delta$  9.08–9.05 (1H, d, ArH), 8.39–8.37 (1H, d, ArH), 8.26–8.21 (3H, m, ArH), 8.17–8.14 (2H, m, ArH), 8.07–8.03 (2H, m, ArH), 2.91 (3H, s,  $\text{CH}_3$ );  $^{13}\text{C}$  NMR (100 MHz,  $\text{CDCl}_3$ ):  $\delta$  202.13, 133.99, 131.89, 131.87, 131.05, 130.49, 129.72, 129.61, 129.47, 127.11, 127.05, 126.38, 126.32, 126.08, 124.98, 124.26, 123.96, 30.46. GC–MS: M, found 244.  $\text{C}_{18}\text{H}_{12}\text{O}$  requires 244.29.

**4.4.2. 4-Pyren-1-yl-pyrimidine (PPM).** To a toluene (20 mL) solution of  $\text{ZnCl}_2$  (0.14 g, 1 mmol), and triethyl ortho-formate (5 mL, 30 mmol) were added AP (2.44 g, 10 mmol), and ammonium acetate (1.54 g, 20 mmol). The mixture was heated at 100 °C under a nitrogen atmosphere for 48 h. A saturated aqueous solution of  $\text{NaHCO}_3$  (100 mL) was added to the mixture to quench the reaction. The mixture was extracted with  $\text{CHCl}_3$ , and the organic extracts were dried over anhydrous  $\text{MgSO}_4$ , filtrated, and concentrated. The crude product was purified by silica gel column chromatography to give the compound PPM (0.59 g, 21%) as light yellow powder.  $^1\text{H}$  NMR (400 MHz,  $\text{CDCl}_3$ ):  $\delta$  9.49 (1H, s, pyrimidine–H), 8.93–8.92 (1H, d, pyrimidine–H), 8.51–8.49 (1H, d, pyrene–H), 8.21–8.04 (8H, m, pyrene–H), 7.80–7.79 (1H, d, pyrimidine–H);  $^{13}\text{C}$  NMR (100 MHz,  $\text{CDCl}_3$ ):  $\delta$  166.84, 159.09, 157.04, 132.49, 132.46, 131.30, 130.74, 128.87, 128.77, 128.64, 127.51, 127.30, 126.34, 125.95, 125.63, 125.05, 124.91, 124.64, 123.95, 122.76; GC–MS: M, found 281.  $\text{C}_{20}\text{H}_{12}\text{N}_2$  requires 280.32.

#### Acknowledgements

This work was financially supported by the National Basic Research Program of China (973 Program, 2009CB930601), the National Natural Science Foundation of China (Project No. 50803027, No. 50903001, No. 20905038), and the Natural Science Fund for Colleges and Universities in Jiangsu Province (Grant No. 08KJD430020).

#### Supplementary data

Supplementary data related to this article can be found online at doi:10.1016/j.tet.2011.12.071.

#### References and notes

- (a) Schrader, T.; Hamilton, A. *Functional Synthetic Receptors*; John Wiley: New York, NY, 2005; (b) Anslyn, E. V. *J. Org. Chem.* **2007**, *72*, 687–699; (c) de Silva, R. A. P.; Gunnlaugsson, T.; McCoy, C. P. *J. Chem. Educ.* **1997**, *74*, 53–58; (d) Bodenant, B.; Weil, T.; Businelli-Pourcel, M.; Fages, F.; Barbe, B.; Pianet, I.; Laguerre, M. *J. Org. Chem.* **1999**, *64*, 7034–7039.
- (a) Nadal, M.; Schuhmacher, M.; Domingo, J. L. *Sci. Total Environ.* **2004**, *321*, 59–69; (b) Fitzgerald, W. F.; Lamgorg, C. H.; Hammerschmidt, C. R. *Chem. Rev.* **2007**, *107*, 641–662; (c) Koester, C. *J. Anal. Chem.* **2005**, *77*, 3737–3754; (d) Richardson, S. D.; Ternes, T. A. *Anal. Chem.* **2005**, *77*, 3807–3838.
- (a) Chen, P.; He, C. *J. Am. Chem. Soc.* **2004**, *126*, 728–729; (b) Ono, A.; Togashi, H. *Angew. Chem., Int. Ed.* **2004**, *43*, 4300–4302; (c) Liu, B.; Tian, H. *Chem. Commun.* **2005**, 3156–3158; (d) Wu, J. S.; Hwang, I. C.; Kim, K. S.; Kim, J. S. *Org. Lett.* **2007**, *9*, 907–910; (e) Nolan, E. M.; Lippard, S. J. *Chem. Rev.* **2008**, *108*, 3443–3480; (f) Chen, X.; Baek, K. H.; Kim, Y.; Kim, S. J.; Shin, I.; Yoon, J. *Tetrahedron* **2010**, *66*, 4016–4021; (g) Mahato, P.; Ghosh, A.; Saha, S.; Mishra, S.; Mishra, S. K.; Das, A. *Inorg. Chem.* **2010**, *49*, 11485–11492; (h) Lohani, C. R.; Kim, J. M.; Lee, K. H. *Tetrahedron* **2011**, *67*, 4130–4136.
- (a) Winnik, F. M. *Chem. Rev.* **1993**, *93*, 587–614; (b) Nishizawa, S.; Kato, Y.; Teramae, N. *J. Am. Chem. Soc.* **1999**, *121*, 9463–9464; (c) Sahoo, D.; Narayanaswami, V.; Kay, C. M.; Ryan, R. O. *Biochemistry* **2000**, *39*, 6594–6601; (d) Kim, S.-J.; Noh, K. H.; Lee, S. H.; Kim, S. K.; Kim, S. K.; Yoon, J.-J. *Org. Chem.* **2003**, *68*, 597–600; (e) Yuasa, H.; Miyagawa, N.; Izumi, T.; Nakatani, M.; Izumi, M.; Hashimoto, H. *Org. Lett.* **2004**, *6*, 1489–1492; (f) Moon, S. Y.; Yoon, N. J.; Park, S. M.; Chang, S. K. *J. Org. Chem.* **2005**, *70*, 2394–2397; (g) Jun, E. J.; Won, H. N.; Kim, J. S.; Lee, K. H.; Yoon, J.

- Tetrahedron Lett.* **2006**, *47*, 4577–4580; (h) Park, S. M.; Kim, M. H.; Choe, J. I.; No, K. T.; Chang, S. K. *J. Org. Chem.* **2007**, *72*, 3550–3553.
- (a) Fabbri, L.; Poggi, A. *Chem. Soc. Rev.* **1995**, *24*, 197–202; (b) Birks, J. B. *Photophysics of Aromatic Molecules*; Wiley Inter-Science: London, 1970.
  - (a) Shiraiishi, Y.; Tokitoh, Y.; Hirai, T. *Org. Lett.* **2006**, *8*, 3841–3844; (b) Kim, H. J.; Hong, J.; Hong, A.; Ham, S.; Lee, J. H.; Kim, J. S. *Org. Lett.* **2008**, *10*, 1963–1966; (c) Jung, H. S.; Park, M.; Han, D. Y.; Kim, E.; Lee, C.; Ham, S.; Kim, J. S. *Org. Lett.* **2009**, *11*, 3378–3381.
  - (a) Kim, J. S.; Choi, M. G.; Song, K. C.; No, K. T.; Ahn, S.; Chang, S. K. *Org. Lett.* **2007**, *9*, 1129–1132; (b) Park, S. Y.; Yoon, J. H.; Hong, C. S.; Souane, R.; Kim, J. S.; Matthews, S. E.; Vicens, J. *J. Org. Chem.* **2008**, *73*, 8212–8218; (c) Zhou, Y.; Zhu, C. Y.; Gao, X. S.; You, X. Y.; Yao, C. *Org. Lett.* **2010**, *12*, 2566–2569; (d) Kumar, M.; Kumar, R.; Bhalla, V. *Org. Lett.* **2011**, *13*, 366–369; (e) Martínez, R.; Espinosa, A.; Tárraga, A.; Molina, P. *Tetrahedron* **2010**, *66*, 3662–3667; (f) Hou, C.; Xiong, Y.; Fu, N.; Jacquot, C. C.; Squier, T. C.; Cao, H. *Tetrahedron Lett.* **2011**, *52*, 2692–2696; (g) Liu, X.; Yang, X.; Fu, Y.; Zhu, C.; Cheng, Y. *Tetrahedron* **2011**, 3181–3186.
  - (a) Caballero, A.; Martínez, R.; Lloveras, V.; Ratera, I.; Vidal-Gancedo, J.; Würst, K.; Tárraga, A.; Molina, P.; Veciana, J. *J. Am. Chem. Soc.* **2005**, *127*, 15666–15667; (b) Martínez, R.; Zapata, F.; Caballero, A.; Espinosa, A.; Tárraga, A.; Molina, P. *Org. Lett.* **2006**, *8*, 3235–3238.
  - (a) Valeur, B.; Leray, I. *Coord. Chem. Rev.* **2000**, *205*, 3–40; (b) Nohta, H.; Satozono, H.; Koiso, K.; Yoshida, H.; Ishida, J.; Yamaguchi, M. *Anal. Chem.* **2000**, *72*, 4199–4202; (c) Okamoto, A.; Ichiba, T.; Saito, I. *J. Am. Chem. Soc.* **2004**, *126*, 8364–8365.
  - (a) Ojida, A.; Mito-oka, Y.; Sada, K.; Humachi, I. *J. Am. Chem. Soc.* **2004**, *126*, 2454–2463; (b) Cao, Y.; Zheng, Q.; Chen, C.; Huang, Z. *Tetrahedron Lett.* **2003**, *44*, 4751–4755; (c) Coskun, A.; Yilmaz, M. D.; Akkaya, E. U. *Org. Lett.* **2007**, *9*, 607–609; (d) Liu, L.; Zhang, G.; Xiang, J.; Zhang, D.; Zhu, D. *Org. Lett.* **2008**, *10*, 4581–4584; (e) Li, Z.; Lou, X.; Yu, H.; Li, Z.; Qin, J. *Macromolecules* **2008**, *41*, 7433–7439; (f) Wan, Y.; Niu, W.; Behof, W. J.; Wang, Y.; Boyle, P.; Gorman, C. B. *Tetrahedron* **2009**, *65*, 4293–4297; (g) Suresh, M.; Mandal, A. K.; Saha, S.; Suresh, E.; Mandoli, A.; Liddo, R. D.; Parnigotto, P. P.; Das, A. *Org. Lett.* **2010**, *12*, 5406–5409.
  - Jain, K. S.; Chitre, T. S.; Miniyaar, P. B.; Kathiravan, M. K.; Bendre, V. S.; Veer, V. S.; Shahane, S. R.; Shishoo, C. J. *Curr. Sci.* **2006**, *90*, 793–803.
  - (a) Wong, K. T.; Hung, T. S.; Lin, Y.; Wu, C. C.; Lee, G. H.; Peng, S. M.; Chou, C. H.; Su, Y. O. *Org. Lett.* **2002**, *4*, 513–516; (b) Wu, C. C.; Lin, Y. T.; Chiang, H. H.; Cho, T. Y.; Chen, C. W. *Appl. Phys. Lett.* **2002**, *81*, 577–579; (c) Hughes, G.; Wang, C.; Batsanov, A. S.; Fern, M.; Frank, S.; Bryce, M. R.; Perepichka, I. F.; Monkman, A. P.; Lyons, B. P. *Org. Biomol. Chem.* **2003**, *1*, 3069–3077; (d) Lin, C. F.; Huang, W. S.; Chou, H. H.; Lin, J. T. *J. Organomet. Chem.* **2009**, *694*, 2757–2769; (e) Ge, G.; He, J.; Guo, H.; Wang, F.; Zou, D. *J. Organomet. Chem.* **2009**, *694*, 3050–3057; (f) Wang, Z. Q.; Xu, C.; Dong, X. M.; Zhang, Y. P.; Hao, X. Q.; Gong, J. F.; Song, M. P.; Ji, B. M. *Inorg. Chem. Commun.* **2011**, *14*, 316–319; (g) Su, S. J.; Cai, C.; Kido, J. *Chem. Mater.* **2011**, *23*, 274–284.
  - Sasada, T.; Kobayashi, F.; Sakai, N.; Konakahara, T. *Org. Lett.* **2009**, *11*, 2161–2164.
  - Simon, J. A.; Curry, S. L.; Schmehl, R. H.; Schatz, T. R.; Piotrowiak, P.; Jin, X.; Thummel, R. P. *J. Am. Chem. Soc.* **1997**, *119*, 11012–11022.
  - Shortreed, M.; Kopelman, R.; Kuhn, M.; Hoyland, B. *Anal. Chem.* **1996**, *68*, 1414–1418.
  - Nolan, E. M.; Racine, M. E.; Lippard, S. J. *Inorg. Chem.* **2006**, *45*, 2742–2749.
  - TPAPM was synthesized from triphenylamine by two steps. The synthetic route for TPAPM and characterization were shown in [supplementary data](#).
  - Hamai, S.; Hirayama, F. *J. Phys. Chem.* **1983**, *87*, 83–89.